Wave energy converter control by wave prediction and dynamic programming

Guang Li[a], George Weiss[b], Markus Mueller[c], Stuart Townley[c], Mike Belmont[a]

[a] *College of Engineering, Mathematics and Physical Sciences, University of Exeter, Harrison Building, North Park Road, Exeter, EX4 4QF, UK*
[b] *Faculty of Engineering, Tel Aviv University, Ramat Aviv 69978, Israel*
[c] *Environment and Sustainability Institute, University of Exeter Cornwall Campus, Cornwall, TR10 9EZ, UK*

Abstract

This paper demonstrates that deterministic sea wave prediction (DSWP) combined with constrained optimal control can dramatically improve the efficiency of sea wave energy converters (WECs), while maintaining their safe operation. A point absorber WEC employing a hydraulic/electric power take off system **is focused on**. Maximising energy take-off while minimising the risk of damage is formulated as an optimal control problem with a disturbance input (the sea elevation) and with both state and input constraints. This optimal control problem is non-convex, which **invalidates direct use of** quadratic programming algorithms for the optimal solution. **It is demonstrated** that the optimum can be achieved by bang-bang control. This paves the way to adopt a dynamic programming (DP) algorithm to resolve the on-line optimization problem efficiently. Simulation results show that this approach is very effective, yielding at least a two-fold increase in energy output as compared to control schemes which do not exploit DSWP. This level of improvement is possible even using relatively low precision DSWP over short time horizons. A key finding is that only about 1 sec of prediction horizon is required, however, the technical difficulties involved in obtaining good estimates necessitate a DSWP system capable of prediction over tens

Email addresses: g.li@exeter.ac.uk (Guang Li), gweiss@eng.tau.ac.il (George Weiss), M.Mueller@exeter.ac.uk (Markus Mueller), s.b.townley@exeter.ac.uk (Stuart Townley), M.R.Belmont@exeter.ac.uk (Mike Belmont)

of seconds.

Keywords: wave energy, constrained optimal control, bang-bang control, dynamic programming, deterministic sea wave prediction

1. Introduction

Ocean waves provide an enormous source of renewable energy [1, 2]. Research into wave energy was initially stimulated by the oil crisis of the 1970s [3]. Since then many different types of sea *wave energy converters* (WECs) have been designed and tested [4, 5], but this is still a relatively immature technology (compared to solar or wind energy) and is far from being commercially competitive with traditional fossil fuel or nuclear energy sources. Progress is hampered by two fundamental problems:

1. Inefficient energy extraction, often due to the fact that the WEC's dynamic parameters are not optimally tuned and their control is not optimal for most wave profiles.

2. Risk of device damage. In order to prevent WECs from being damaged by large waves, they have to be shut down, especially during winter storms. Such periods of inactivity can last for days.

Extracting the maximum possible time average power from WECs, while reducing the risk of device damage involves a combination of good fundamental engineering design of the devices and effective control of their operation. The traditional approach to these issues exploits short term statistical properties of the sea [6] but it has been shown [7, 8] that doing so severely limits the average power that can be extracted. **The above two problems are addressed** by considering schemes designed to achieve optimal control. It will be shown that (as [9–11] demonstrated in the 1970s) methods for achieving the maximum power output are inevitably non-causal and require prediction of the shape of the incident waves. The recent development of *deterministic sea wave prediction* (DSWP) as a scientific discipline [12–28], particularly real time DSWP [12–19, 26, 28] now makes such an approach realistic. For a variety of reasons high accuracy real time DSWP is very demanding. However it will be shown that the optimal control techniques described here provide considerable improvements over traditional WEC control methods, even with modestly accurate DSWP and relatively short prediction horizons.

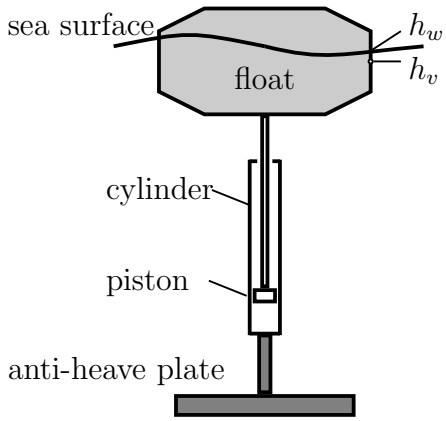

Figure 1: Schematic diagram of the point absorber

The dimensions of point absorbers are small compared with the wavelength of incoming waves and they are potentially very efficient if their frequency response function closely matches the spectrum of the incident waves (resonance). Passive control methods (such as impedance matching) have been explored to improve energy extraction by tuning the dynamical parameters of the devices [9, 29–31]. Most of these approaches are linear control schemes. A non-linear control method that has received some attention is latching, [32–37]. This attempts to force the phase angle between the float and the wave at the WEC to be similar to conditions at resonance. The above control strategies do not use prediction of the forces acting on the WEC and thus inevitably lead to sub-optimal energy extraction. Since the early work [5, 9, 11] there have been a number of authors who have recognized the importance of DSWP in the control of a variety of floating body applications [7, 8, 17, 37, 38], but these have, as yet, not been incorporated into actual control schemes.

The point absorber model used is shown in Fig. 1 and roughly corresponds to the Power Buoy device PB150 developed by OPT Inc, see [39]. On the sea surface is a float, below which hydraulic cylinders are vertically installed. These cylinders are attached at the bottom to a large area anti-heave plate whose vertical motion is designed to be negligible compared to that of the float. The heave motion of the float drives the pistons inside the hydraulic cylinders to produce a liquid flow. The liquid drives hydraulic motors attached to a synchronous generator. From here, the power reaches the grid via back-to-back AC/DC/AC converters. The mechanical circuit corre-

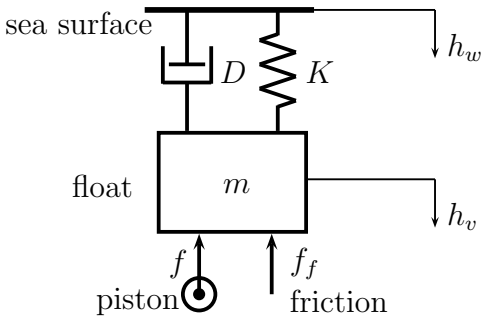

Figure 2: A mechanical circuit representation of the point absorber

sponding to this simplified model is shown in Fig. 2. Here h_w is the water level, h_v is the height of the mid-point of the float and D is the hydrodynamic damping of the float including added damping due to the damping effect of the movement of the float [1]. K is the hydrostatic stiffness giving the buoyancy force, which can be calculated from the float geometry, while m is the mass of the float including "added mass" [1]. The friction force acting on the float is $f_f = D_f \dot{h}_v$. In order to simplify the model the frequency dependence of both D and m **is neglected** (see, e.g., [29]). The static component of the friction force f_f **is also neglected**. For a more thorough investigation of the modeling issues of point absorbers, see [1, 40, 41].

The control input is the q-axis current in the generator-side power converter, to control the electric torque of the generator. The generator torque is proportional to the force f acting on the pistons from the fluid in the cylinders. Since the motion of the float imposes a velocity v on the piston, the extracted power $P(t)$ at time t is expressed as

$$P(t) = f(t)v(t). \tag{1}$$

This power is smoothed by the capacitors on the DC link of the converters. **In the model in this paper**, the modest power losses in the hydraulic transmission, the generator and the converters will be neglected.

To avoid damage, and for overall performance reasons, two constraints have to be considered in any real WEC. One concerns the relative motion of the float to the sea surface (it should neither sink nor raise above the water and then slam), which can be expressed as

$$|h_w - h_v| \leq \Phi_{\max}. \tag{2}$$

The other constraint is on the control signal set by limitations on the allowable converter current. This constraint can be expressed as

$$|f| \leq \gamma. \tag{3}$$

The control objective is to maximize the extracted energy subject to the constraints (2) and (3). **Note that** there is further constraint on the motion of the float because of the limited excursion of the piston with respect to the cylinder (see Fig. 1). This constraint has the form $|h_v| \leq \lambda$. However, **this constraint should not be considered**, since λ **is assumed large enough** compared to the expected excursion.

The constraints imposed on WECs significantly affect the power that can be extracted. It has been shown that by using control strategies that incorporate these constraints, considerable increases in the energy output can be obtained without increasing the risk of damage [7, 8]. The ability to handle constraints combined with the development of real-time wave prediction methods has recently led to an interest in the use of *model predictive control* (MPC) for wave energy devices [42–44]. The work published to date has used standard MPC techniques and they rely on the formulation of a convex *quadratic programming* (QP) problem. The underlying problem formulations and the cost function representations in [42–44] differ from **the case in this paper**. **The question is left open** if the convexity assumption holds for a broad class of constrained optimal control problems for WECs. However, this assumption does not hold for the problem formulated in this paper and many other similar optimal control problems [45, 46].

In this paper, the constrained optimal control problem is solved using fundamental principles from optimal control theory [47–49], see Section 3, and real time deterministic sea wave prediction [12–19, 26, 28]. It is demonstrated that the optimal control is of bang-bang type, meaning that the control input f is always at one edge of the allowed range, see Subsection 3.2. As will be shown, for an arbitrary sea wave input known over an interval of time (not a sine wave), direct numerical computation of the optimal control scheme is not realistic. Consequently, *dynamic programming* (DP) [45], which is well suited for constrained optimal control problems [50], **is employed**. Some detail is sacrificed in the hydrodynamic modelling, leading to a model of manageable complexity for on-line DP.

The implementation of DP on a WEC control system is based on the assumption that the sea surface shape can be predicted for a short time period.

This requirement has been a bottleneck for the development of suitable optimal control strategies for WECs. However, the developments in deterministic sea wave modeling techniques have made real time sea wave prediction for a short time period realizable, [12–19, 26, 28]. A key finding from this work is that the prediction horizons required are considerably smaller than those resulting from the previous studies [42–44].

For the sake of comparison, simulations have also been performed for various non-prediction-based WEC control strategies. The results demonstrate the following benefits of the approach **proposed in this paper**. 1) Significant increase in energy output. **Up to a two-fold increase is achieved** in energy output when compared to nearest rivals which do not exploit sea state prediction. 2) Robustness to the accuracy and prediction horizon of DSWP. Especially important is the possibility of reducing the prediction horizon, because the difficulties associated with real time DSWP increase significantly with the prediction horizon.

The structure of the paper is as follows. Section 2 formulates the constrained optimal control problem for the WEC. Section 3 provides a detailed analysis for this optimal control problem. The dynamic programming control strategy is developed in Section 4, and compared in simulation with several other control methods in Section 5.

2. The WEC model

It is convenient to replace the mechanical circuit in Fig. 2 with its electrical equivalent, shown in Fig. 3. The relationship between the electrical and mechanical elements from Figures 2 and 3 is:

$$R = \frac{1}{D}, \qquad L = \frac{1}{K}, \qquad m = C, \qquad R_f = \frac{1}{D_f}.$$

Moreover, force and velocity in Fig. 2 correspond to current and voltage in Fig. 3. Hence, w and v are voltages associated with the vertical velocities of the sea level and float, respectively; the current i_L corresponds to the spring force in Fig. 2; the current through R_f corresponds to the friction force between the float and the lower part of the WEC that is rigidly connected to the heave plate. The control input u is the current associated with the control force f in Fig. 2 (numerically, they are the same).

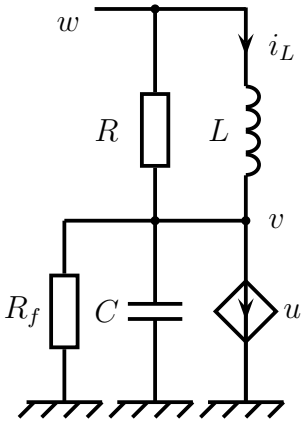

Figure 3: The equivalent electric circuit representation of the WEC

From the circuit, the following state space model holds

$$\begin{bmatrix} \frac{di_L}{dt} \\ \frac{dv}{dt} \end{bmatrix} = \begin{bmatrix} 0 & -\frac{1}{L} \\ \frac{1}{C} & -\frac{1}{C}(\frac{1}{R} + \frac{1}{R_f}) \end{bmatrix} \begin{bmatrix} i_L \\ v \end{bmatrix} + \begin{bmatrix} \frac{1}{L} \\ \frac{1}{RC} \end{bmatrix} w + \begin{bmatrix} 0 \\ -\frac{1}{C} \end{bmatrix} u. \tag{4}$$

The extracted energy in the time interval $[0, T]$ is $E = \int_0^T vu \, \mathrm{d}t$. The two constraints corresponding to (2) and (3) can be expressed as $|i_L| \leq \delta$ and $|u| \leq \gamma$, respectively, where $\delta = \Phi_{\max}/L$.

If the constraint $|i_L| \leq \delta$ is violated, which means that the float moves outside some acceptable limit with respect to the water surface, then the incremental buoyancy force gets much smaller, due to the smaller cross-section of the buoy at the water level, and a nonlinearity is introduced into the WEC model. Φ denotes the magnetic flux of the inductor, which corresponds in the mechanical circuit to the vertical displacement difference between the water level and the mid-point of the float $\Phi(t) = \int_0^t (w - v) \, \mathrm{d}\tau$. Then the nonlinear behavior of the inductor can be approximated by

$$i_L = \begin{cases} \Phi_{\max}/L + (\Phi - \Phi_{\max})/kL, & \text{if } \Phi > \Phi_{\max} \\ \Phi/L, & \text{if } |\Phi| \leq \Phi_{\max} \\ -\Phi_{\max}/L + (\Phi + \Phi_{\max})/kL, & \text{if } \Phi < -\Phi_{\max} \end{cases} \tag{5}$$

where $k > 1$ is a constant and $\Phi_{\max} = L\delta$.

3. The WEC optimal control problem

3.1. Problem formulation

Introducing the state vector $x = [i_L \; v]^\top$ allows (4) to be rewritten as

$$\dot{x} = A_c x + B_{cu} u + B_{cw} w, \tag{6a}$$

$$v = C_c x\,, \qquad C_c = [0 \; 1]\,. \tag{6b}$$

The control objective is to maximize the energy $E = \int_0^T v(t)u(t)\,\mathrm{d}t$ extracted over a time interval $[0, T]$, assuming that the disturbance input w is known. The following constraints must also be satisfied (for all $t \in [0, T]$):

$$|x_1| \le \delta\,, \qquad |u| \le \gamma\,. \tag{7}$$

Thus, the optimization problem is

$$\text{maximize } E \;\text{ subject to }\; (7). \tag{8}$$

Note that if the constraints (7) were removed and if w were a sine wave then, for large T, this would become an impedance matching problem, which has an simple analytic solution. If w is not a sine wave, and it is not known in advance, then this "solution" becomes non-causal [1] and various causal approximations to it have been studied in [51–54].

3.2. Optimal control analysis

In the following analysis, problem (8) is recast by introducing the cost functional

$$J_\varepsilon(u) = \int_0^T \left[-v(t)u(t) + \frac{\varepsilon}{\delta - |x_1(t)|} \right] \mathrm{d}t \tag{9}$$

where, for some (small) $\varepsilon > 0$, the penalty term $\frac{\varepsilon}{\delta - |x_1(t)|}$ replaces the state constraint [55]. The modified cost function is more conservative than (8), because $\frac{\varepsilon}{\delta - |x_1(t)|} \to \infty$ as $|x_1(t)| \to \delta$. Put

$$\mathcal{U} = \{u\colon [0, T] \to [-\gamma, \gamma] \;\big|\; u \text{ measurable}\}\,,$$

then the problem is to minimize $J_\varepsilon(u)$ with respect to $u \in \mathcal{U}$ subject to x, v being the solution of (6). It is known that for $\varepsilon \to 0$ ($\varepsilon > 0$) the solution of the above unconstrained (in state) optimal control problem converges to the solution of the constrained optimal control problem (8), see [55].

To solve the optimization problem for J_ε, Pontryagin's Minimum Principle ([47, Ch. 1], [48] or [49]) **is used**. **First introduce** the pre-Hamiltonian

$$H(t,x,\lambda,u) = L(t,x,u) + \lambda^\top (A_c x + B_{cu} u + B_{cw} w) \tag{10}$$

where $L(t,x,u) = -y(t)u(t) + \varepsilon/(\delta - |x_1(t)|)$ is the integrand of $J_\varepsilon(u)$, see (9), and $\lambda = [\lambda_1 \ \lambda_2]^\top$ denotes the co-state. Recall that the co-states λ_1, λ_2 satisfy the differential equation [47, p. 18]

$$\frac{\mathrm{d}\lambda_i}{\mathrm{d}t} = -\frac{\partial H}{\partial x_i}, \qquad i = 1, 2. \tag{11}$$

Using the notation $R_p = \frac{RR_f}{R+R_f}$, **the pre-Hamiltonian becomes** (by a short computation)

$$H(t,x,\lambda,u) = -\left[y(t) + \frac{\lambda_2(t)}{C}\right] u(t) + \frac{\varepsilon}{\delta - |x_1(t)|}$$

$$+\frac{\lambda_1(t)}{L}(w(t) - y(t)) + \frac{\lambda_2(t)}{C}\left(x_1(t) + \frac{w(t)}{R} - \frac{y(t)}{R_p}\right).$$

Pontryagin's minimum principle states that if u^* is the optimal input and x^*, λ^* are the optimal state and co-state trajectory, then u^* minimizes H:

$$H\big(x^*(t), u^*(t), \lambda^*(t), t\big) \le H\big(x^*(t), u_0, \lambda^*(t), t\big)$$

for all $t \in [0,T]$ and all $u_0 \in [-\gamma, \gamma]$. Since H is linear in u, its minimum with respect to u is always achieved at $u = \gamma$ or at $u = -\gamma$. More precisely,

$$u^*(t) = \begin{cases} \gamma & \text{if } y(t) + \dfrac{\lambda_2(t)}{C} > 0, \\ -\gamma & \text{if } y(t) + \dfrac{\lambda_2(t)}{C} < 0. \end{cases} \tag{12}$$

If $y(t) + \frac{\lambda_2(t)}{C} = 0$ then the minimum principle does not give $u^*(t)$, but the times when this happens are negligible (they form a set of measure zero).

This type of control, jumping between a finite number of extreme points, is called "bang-bang control". To find u^* the sign of $y(t) + \dfrac{\lambda_2(t)}{C}$ for all $t \in [0,T]$ **has to be determined**. The function

$$H_0(t,x,\lambda) = \min_{u_0 \in [-\gamma,\gamma]} H(t,x,\lambda,u_0)$$

is called the Hamiltonian. **Here**

$$H_0(t,x,\lambda) = \mp\left[v(t)+\frac{\lambda_2(t)}{C}\right]u_{\max} + \frac{\varepsilon}{\delta-|x_1(t)|} + \frac{\lambda_1(t)}{L}(w(t)-v(t)) + \frac{\lambda_2(t)}{C}\left(x_1(t)+\frac{w(t)}{R}-\frac{v(t)}{R_p}\right).$$

According to Pontryagin's minimum principle, along an optimal trajectory the system evolves according to the canonical equations

$$\dot{x} = \frac{\partial H_0}{\partial \lambda}, \qquad \dot{\lambda} = -\frac{\partial H_0}{\partial x},$$

with terminal condition $\lambda(T) = 0$ as there is no terminal cost in the functional J_ε. Thus, to find the optimal control it is necessary to solve the two-point boundary value problem

$$\begin{aligned}
\dot{x}_1 &= -\frac{1}{L}x_2 + \frac{1}{L}w \\
\dot{x}_2 &= \frac{1}{C}x_1 - \frac{1}{R_pC}x_2 \mp \frac{1}{C}\gamma + \frac{1}{RC}w \\
\dot{\lambda}_1 &= \frac{\pm\varepsilon}{(\delta-|x_1|)^2} - \frac{\lambda_2}{C}, \qquad (+ \text{ sign if } x_1(t) < 0) \\
\dot{\lambda}_2 &= \pm\gamma + \frac{\lambda_1}{L} + \frac{\lambda_2}{RC}, \\
& x_i(0) = x_i^0, \quad \lambda_i(T) = 0,\ i = 1,2,
\end{aligned}$$

where the sign before γ is taken from the input $u(t)$ for every $t \in [0,T]$, which, in view of (12), is determined by the sign of $x_2(t) + \frac{\lambda_2(t)}{C}$. The sea surface velocity w may be considered as a disturbance signal.

This problem must be solved numerically and unlike for initial value problems, where forward stepping can be used, here some form of iteration scheme is necessary (so called shooting methods). This is computationally expensive and the problem is ill conditioned. Therefore, instead of numerically solving the two point boundary value problem, the optimal control will be approximated using discretization and DP, see Section 4. This makes it possible to compute the discretized control input step by step without having to solve the canonical equations. However, Pontryagin's minimum principle is still important for **showing** that the optimal control is of bang-bang type, which dramatically simplifies the DP algorithm.

3.3. Sea-wave model and wave prediction

The computational cost of real time DSWP methods for short-crested waves forces the sea-wave model to be a linear superposition of a number of long-crested swells, which is the conventional oceanographic wave model [6]. Additionally, it is assumed that the sea surface is statistically stationary over the timescale of the prediction process (typically a few minutes). At the WEC site the wave height at a position $(x, y) \in \mathbb{R}^2$ and at time $t \in \mathbb{R}$ is described by

$$h(t, x, y) = \sum_{m=1}^{M} \sum_{n=1}^{N} A_{n,m} \cos(\kappa_n d_m(x, y) - \omega_n t + \Phi_{n,m}),$$

where, for fixed $m \in \{1, \dots M\}$, the sum $\sum_{n=1}^{N} A_{n,m} \cos(...)$ describes one particular long-crested swell/wave front. Here $N \in \mathbb{N}$ is the number of frequencies ω_n, the wave number is $\kappa_n = 2\pi/\lambda_n$ where λ_n is the wave length, $d_m(x, y)$ is the "distance" of the point (x, y) to the m^{th} wave front passing through the origin ($d_m(x, y)$ may be negative) and $\Phi_{n,m}$ is a phase-shift. **Approximately,** $\kappa_n \approx \omega_n^2/g$ **holds**, where g is the gravity constant. The precise relationship depends also on the depth of the water.

One form of real time DSWP [12–19] involves two steps: (1) determine the continuously updated directions of component waves (typically this uses a few minutes of data) and (2) for a particular wave profile (typically requires 30 seconds of data) find the particular parameters $A_{n,m}$ and $\Phi_{n,m}$. Using the wave directions and the magnitudes and phases allows the short wave profile to be predicted when it has propagated to the prediction site. This approach to real time DSWP for short crested waves requires some form of remote sensing technology such as wave LIDAR [56], or an array of wave buoys.

4. Dynamic Programming for WEC control

4.1. A brief introduction to dynamic programming

Dynamic programming (DP), originally developed by [45], is a powerful approach for numerically solving discrete optimization problems [46]. It is a multi-stage decision process based on Bellman's principle of optimality [45]. Based on this principle, the process of making a decision **can be simplified** by breaking the process down into a sequence of decision steps.

DP has also long been recognized as being naturally suited for resolving a wide variety of optimal control problems [46, 57]. This is mainly because

it allows diverse forms of the criterion functions and broad classes of systems to be controlled, which can be nonlinear and time varying.

The DP optimization procedure is briefly described as follows. The first step is to discretize the continuous system model, $\dot{x} = f(x, u, w, t)$ to its discrete time form $x(k+1) = g(x(k), u(k), w(k), k)$ and quantize each state variable $x_i(k)$ and each control variable $u_i(k)$. The second step is to define a sequence of criterion functions $J_k(y, u)$, $k = 1, \ldots N$, representing the performance values (energy in the present work) from the time k to the final time N for all admissible inputs $u(i)$, outputs $y(i)$ and states $x(i)$, $i = k, \ldots N$, that satisfy the system's dynamic equations. The third step is to find the optimal control sequence in a recursive manner. The conventional computational procedure of the DP algorithm starts with determining the optimal values of J_N obtained at the final stage N for all possible states and control inputs. Then the optimal values J_k, $k = 1, \ldots, N$, can be found backwards by a recurrence relationship. The crucial point of the algorithm is that since the optimal values of J_{k+1} for all required states of the system have already been calculated in the previous step, only one stage of optimization is required for obtaining the optimal value of J_k. This is very efficient. When this recursive calculation procedure finishes at the initial stage $k = 1$, the optimal value of J_1 for the whole process and the corresponding optimal control sequence at each quantized initial state can be determined. Because this DP algorithm performs the calculation recursively from the last stage backward to the initial stage, it is usually called *backward dynamic programming* (BDP).

4.2. Implementation of dynamic programming for optimal control

Optimal control based on DP can be implemented off-line or on-line, according to the characteristics of the control problem. Some optimal control problems can be solved by running the BDP algorithm off-line and storing in memory the optimal control values for all the quantized initial states. At each sampling instant, the control signal is generated by looking up the memory based on the measured or estimated state. Using this off-line method, the real-time implementation speed can be very fast, because the main computational burden is removed to off-line.

In the on-line implementation of the DP algorithm for WECs, at each sampling instant, the DP algorithm determines the optimal control input to achieve maximal energy extraction for the WEC over the prediction horizon, while satisfying input and state constraints. Denote the sampling period by

T_s. Then the N-stage receding horizon is $t_0 + H_p$, where $H_p = N \times T_s$ is the prediction time and t_0 is the present time. The receding horizon slides forward by one sampling period after each execution of the algorithm. At t_0, the DP algorithm produces an optimal control input sequence for the interval $[t_0, t_0 + H_p]$; however, the control action which is applied to the system is only the first value (at time t_0) of this control input sequence. The next execution of the algorithm computes the optimal input for the system within the interval $[t_0 + T_s, t_0 + H_p + T_s]$, with updated sea surface/wave prediction, but only the control input value at $t_0 + T_s$ is applied to the system, and so forth. This on-line optimization control method is known as *model predictive control* (MPC), and also as moving horizon control [58, 59].

For this on-line implementation of the DP algorithm in the WEC control, *forward dynamic programming* (FDP) is better suited than BDP. The FDP algorithm is also based on the principle of optimality, but it calculates the cost by sweeping from the initial stage to the last stage. There are two reasons for adopting FDP as an on-line optimization algorithm. First, FDP can significantly reduce the on-line computational burden. In FDP, at each sampling instant only the optimal control signal corresponding to one initial state is calculated, i.e., the state measured at the present time. In BDP, the optimal control signal is calculated at each possible grid point. Hence the on-line computational speed and memory storage space for FDP are significantly reduced compared with the BDP. Second, in FDP there is no constraint imposed on the final state.

4.3. The FDP algorithm for WEC control

4.3.1. Problem setup

In view of the recursive nature of the FDP, it is first necessary to discretize the WEC's continuous time model (6). The discretized model is

$$x(k+1) = A_d x(k) + B_{du} u(k) + B_{dw} w(k), \tag{13a}$$

$$y(k) = C_d x(k). \tag{13b}$$

Corresponding to the input and state constraints (7), the control input and the state are constrained in the sets $\mathbb{U}$ and $\mathbb{X}$, respectively:

$$\mathbb{U} := \{u \in \mathbb{R} | -\gamma \leq u \leq \gamma\}, \tag{14}$$

$$\mathbb{X} := \{x \in \mathbb{R}^2 | -\delta \leq x_1 \leq \delta\}. \tag{15}$$

Given a predicted wave velocity sequence $\mathbf{w}(N) = \{w(0), \ldots w(N-1)\}$ and a measured initial state $x(0) \in \mathbb{R}^2$, DP aims to resolve the following constrained optimization problem:

$$\begin{aligned} &\min_{\mathbf{u}} \sum_{k=0}^{N-1} [-y(k)u(k)] \quad \text{subject to (13)} \\ &x(k) \in \mathbb{X} \ \text{ for } k = 0, \ldots N-1, \\ &u(k) \in \mathbb{U} \ \text{ for } k = 0, \ldots N-1. \end{aligned} \tag{16}$$

4.3.2. Quantization

An essential step in performing DP optimization within reasonable computational limits is to quantize the state space $\mathbb{X}$ and the input space $\mathbb{U}$. **It is assumed** that u can only take one of the two boundary values of $\mathbb{U}$, $-\gamma$ and γ. This is a reasonable assumption in view of the analysis in Section 3.

The quantization of the two-dimensional state space is shown in Appendix A. Note that in the algorithm, it is not necessary to perform the state quantization physically, since the only purpose of the state quantization is to divide the state space into equivalence classes over which the minimum costs are compared [46]; this will be explained in Subsubsection 4.3.4. For a system with a higher state dimension, more sophisticated quantization methods should be used, see [60].

4.3.3. DP recurrence relation

For every $k \in \{1, 2, \ldots N\}$, **denote** $\mathbf{u}(k) = (u(0), u(1), \ldots u(k-1))$. To proceed the DP optimization, it is necesary to derive the recurrence relation. Define, for $k \geq 1$, the cost function J_k from the initial state $x(0)$ to the present time k by

$$J_k(\mathbf{u}(k)) = \sum_{i=0}^{k-1} [-y(i)u(i)] \tag{17}$$

which depends on $\mathbf{u}(k)$. Note that the sequences of states $(x(0), \ldots, x(k))$ and outputs $(y(0), \ldots, y(k))$ are uniquely determined by the input sequence $\mathbf{u}(k)$, the initial state $x(0)$ and the wave velocity sequence $\mathbf{w}(N)$. Define, for $k = 1, 2, \ldots N$, the minimum cost $I_k(x)$ from the initial state $x(0)$ to any reachable present state x by

$$I_k(x) = \min_{\mathbf{u}(k)} \big\{ J_k(\mathbf{u}(k)) \mid x(k) = x \big\} \tag{18}$$

and set $I_0 = 0$. This function $I_k(x)$ is defined only for those states x that can be reached from $x(0)$ without violating the constraints (7) and the minimum is taken over those input sequences $\mathbf{u}(k)$ for which the constraints remain satisfied up to the time k. According to (13), a reachable state x at time k can be reached from possibly several states z at time $k-1$ using the input $u(k-1)$ at time $k-1$, if they satisfy

$$x = A_d z + B_{du} u(k-1) + B_{dw} w(k-1)\,. \tag{19}$$

Note that, since A_d is invertible and $w(k-1)$ is given, this determines z as a function of x and $u(k-1)$. The function I_k satisfies the recurrence relation

$$I_k(x) = \min_{u(k-1)} \big\{ -(C_d z)u(k-1) + I_{k-1}(z) \mid \text{ (19) holds} \big\}\,. \tag{20}$$

The minimum is taken over all values $u(k-1) \in [-\gamma, \gamma]$ for which z resulting from (19) is also a reachable state.

Using (18), (20) is proved:

$$\begin{aligned} I_k(x) &= \min_{\mathbf{u}(k)} \left\{ -y(k-1)u(k-1) + \sum_{i=0}^{k-2} [-y(i)u(i)] \;\middle|\; x(k) = x \right\} \\ &= \min_{u(k-1)} \min_{\mathbf{u}(k-1)} \left\{ -(C_d z)u(k-1) + \left\{ \sum_{i=0}^{k-2} [-y(i)u(i)] \;\middle|\; x(k-1) = z \right\} \;\middle|\; \right. \\ &\qquad\qquad \left. z \text{ is such that (19) holds} \right\} \\ &= \min_{u(k-1)} \big\{ -(C_d z)u(k-1) + I_{k-1}(z) \mid \text{ (19) holds} \big\}. \end{aligned}$$

4.3.4. Summary of the DP computation procedure

At stage k, for each possible state vector $x(k)$ within the quantized state space, equation (13a) is used to compute all feasible states $x(k+1)$ by applying the wave signal input $w(k)$ and each of the two possible control input values $u(k) = \gamma$ and $u(k) = -\gamma$.

The DP optimization procedure is started at the initial stage $k = 0$ with initial condition $x(0)$ and cost function $I_0 = 0$. Then in view of the recurrence relation (20), compute $I_1 = \min_{\mathbf{u}(1)} \{-y(0)u(0) + I_0\}$, $I_2 = \min_{\mathbf{u}(2)} \{-y(1)u(1) + I_1\}$ and so on until

$$I_N(x) = \min_{\mathbf{u}(N)} \big\{ -y(N-1)u(N-1) + I_{N-1}(z) \mid \text{ (19) holds with } k = N \big\}$$

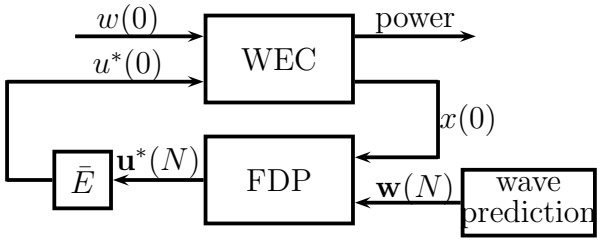

Figure 4: Block diagram for WEC control using FDP (0 stands for the present time)

is reached. Note that the sequence $w(k)$ is used in the above iterations to compute the output sequence $y(k)$ via the system dynamics (13).

Since it is not possible to guarantee that the next state $x(k+1)$ is exactly on a grid point, it is necessary to associate the state with the nearest quantized state. This associating procedure is given in Appendix B.

After associating all the possible values of the state $x(k+1)$ with their nearest quantized states, a comparison is made, based on the recurrence relation (20), to find the minimum cost from the initial stage to the present stage. If several state values are associated with the same quantized state, only the control signal and the index of the state corresponding to the minimum cost are recorded. If some state is driven outside the state constraint, then a large constant value $r > 0$ is added on to the cost function to penalize the state constraint violation, i.e. I_k is set to $I_k + r$. Note that at each stage and each reached state, the true values of the state and cost are recorded. This iteration can be continued until the last stage is reached. At the last stage, the state associated with the minimum cost is searched. Then by tracing back from this final state, the optimal control sequence and the optimal state trajectory can be derived.

4.4. The implementation of the FDP for WEC control

In summary, the implementation for WEC control based on the FDP can be represented by the framework shown in Fig. 4, where $\bar{E} = [1, 0, \ldots 0]$ is used to extract the first control value $u^*(0)$ of the control sequence $\mathbf{u}^*(N)$. At each sampling instant, the WEC control is given as the following procedure:

Step 1 Predict the sea wave magnitude and speed for the next N steps, i.e. the values of $w(k)$ with $k = 0, \ldots N-1$;

Step 2 Implement the DP algorithm using the measured state value $x(0)$

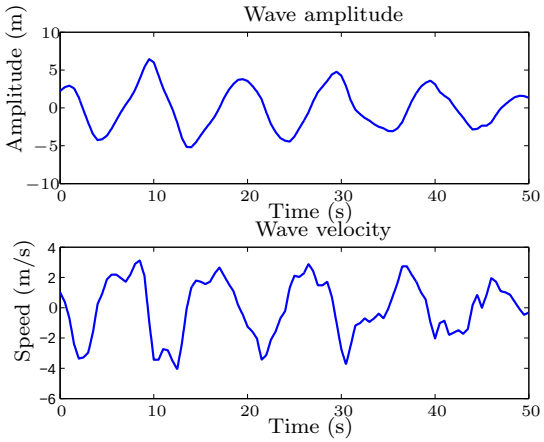

Figure 5: The wave amplitude and velocity data used in the simulations

and $w(k)$ with $k = 0, \ldots N-1$, which is estimated in Step 1; an optimal control sequence $\mathbf{u}^*(N) = \{u^*(0), u^*(1), \ldots u^*(N-1)\}$ is determined;

Step 3 Implement only the first control of $\mathbf{u}^*(N)$, i.e., $u^*(0)$, on the WEC for one sampling period T_s;

Step 4 At the next sampling instant, repeat the procedure from the Step 1.

5. Numerical simulation

The numerical parameters used approximately reflect those of a moderate sized point absorber such as the PB150, but are not intended to be a precise description of any actual system. The float diameter is $d = 9$ m. The height of the float is $\Delta h = 2.4$ m, hence the range of the float heave motion is $[-1.2, 1.2]$m. The sea water density is $\rho = 1025$ kg/m^3. The gravity constant is 9.8 N/kg. The stiffness is $K = \pi(d/2)^2\rho g = \pi \times (9/2)^2 \times 1025 \times 9.8 = 6.39 \times 10^5$ N/m. The mass of the float is $m_s = 10 \times 10^3$ kg. For a circular cylinder, the added mass is equivalent to the displaced mass of the sea water [61]. Here the added mass **is estimated** to be 7×10^4 kg. Then the total mass is $m = m_a + m_s = 8 \times 10^4$ kg. The damping coefficient is taken as $D = 2 \times 10^4$ Nm/s. The damping ratio corresponding to the friction is $D_f = 2 \times 10^4$ Nm/s. In the simulations, $\Phi_{\max} = 1.2$ m. The coefficient k for the nonlinearity of the inductor is chosen as $k = 4$. The maximum control

Table 1: Parameters used for the WEC control system modelling

Description	Notation	Values
Density of sea water	ρ	1025 kg/m^3
Gravity	g	9.8 N/kg
Diameter	d	9 m
Height	Δh	2.4 m
Maximum heave motion	$\Phi_{\max}$	1.2 m
Damping	D	2×10^5 Nm/s
Damping (friction)	D_f	2×10^5 Nm/s
Float mass	m_s	10×10^3 kg
Added mass	m_a	70×10^3 kg
Stiffness	K	6.39×10^5 N/m
Maximum input magnitude	γ	3×10^5 N

input is chosen to be $\gamma = 3 \times 10^5$ N. These parameters are summarized in Table 1.

Real sea wave data gathered off the coast of Cornwall, UK is used. The sea level and velocity for a period of 50 sec used for simulations in this paper are shown in Fig. 5.

The electrical circuit shown in Figure 3 is used as the plant model to be controlled. This model is discretized by an "exact discretization" with a sampling time of $T_s = 0.04$ sec (this means that a zero order hold **is added** at the inputs and a sampler at the output, both working with the period T_s). The discrete time model is of the form (13), with

$$A_d = \begin{bmatrix} 0.9937 & -2.5254 \times 10^4 \\ 4.9398 \times 10^{-7} & 0.9739 \end{bmatrix} \qquad B_{du} = \begin{bmatrix} 6.3412 \times 10^3 \\ -4.9398 \times 10^{-7} \end{bmatrix}$$

$$B_{dw} = \begin{bmatrix} 2.5380 \times 10^4 \\ 1.6221 \times 10^{-2} \end{bmatrix} \qquad C_d = \begin{bmatrix} 0 & 1 \end{bmatrix}$$

In the dynamic programming algorithm, the ranges for the quantization of x_1 and x_2 are [-1200, 1200] and [-7, 7] respectively, and the number of grid points on x_1 and x_2 are $N_{x_1} = N_{x_2} = 50$.

MATLAB$^{\text{TM}}$ and SIMULINK$^{\text{TM}}$ **was used** to perform the simulations, but real-time code would be written in a language such as C combined with dedicated hardware realized functions. The continuous time model of the WEC is built using SIMULINK$^{\text{TM}}$. The FDP algorithm is written in m-code

and then embedded into an S-function to suit the use of SIMULINK^{TM}. The simulations are run on a PC with Intel© Core^{TM} i7 CPU at 2.8 GHz and with 6.0 GB memory. Denote the computational time for performing the FDP algorithm at one sampling instant by T_c, then $T_c \propto N \times N_{x1} \times N_{x1}$. When $N_{x_1} = N_{x_2} = 50$ and $N = 25$, $T_c \approx 0.068$ sec. Although T_c is a bit larger than the sampling period $T_s = 0.04$ sec, this will improve considerably when the algorithm will be written in C and compiled into an executable code on a dedicated processor.

The BDP algorithm was also implemented in the same setting as the FDP for comparison. **It is** found that the BDP algorithm is approximately 8 times slower than the FDP algorithm for most of the simulations in this paper, although BDP yields the same control performance as FDP. In the sequel, only the results obtained by FDP **are shown**.

5.1. DP control and a comparison with other control strategies

In this subsection, two sets of simulations with the prediction horizon for DP control fixed as $H_p = 1$ sec, i.e. $N = 25$ (**it will be shown** why this horizon is chosen in the next subsection) **are presented**. Firstly, it is assumed that the FDP algorithm is implemented when the future wave profiles can be perfectly predicted without any prediction error. Secondly, since the sea wave prediction error is unavoidable, it is assumed that, at each sampling instant, the standard deviation of the prediction error increases, due to the fact that the longer the prediction time, the worse the prediction accuracy. Fig. 5 shows the example of wave speed used in the simulations, over a time interval of 50 sec. In the simulation, the predicted wave data for the DP algorithm is created by adding a sequence of prediction errors e_k to the real wave speed data at each sampling instant from the present time to the end of the prediction time. This e_k is generated by $e_k = \lambda e_{k-1} + w_k$, with $k = 1, 2, \ldots N$. Here w_k is Gaussian white noise, $w_k \sim \mathcal{N}(0, 0.1)$ and the initial value of e_k is $e_0 \sim \mathcal{N}(0, 0.8)$. $\lambda = 1.001$ **is taken**, making the filter unstable, to match with realistic prediction errors that grow as the prediction time grows. The values taken are deliberately very conservative (i.e., in a real application the prediction errors to be smaller **is expected**) [12]. Note that e_0 is not zero; see Section 5.2 for an explanation.

To demonstrate the effectiveness of the DP control, its performance is compared with two alternative control strategies:

a) Linear control:

$$u(k) = \begin{cases} \gamma, & \text{if } Fy(k) > \gamma; \\ Fv(k), & \text{if } -\gamma \leq Fv(k) \leq \gamma; \\ -\gamma, & \text{if } Fy(k) < -\gamma. \end{cases} \tag{21}$$

where F is a constant feedback gain and v is the voltage associated with the vertical velocity of the buoy.

b) Bang-bang control:

$$u(k) = \begin{cases} \gamma, & \text{if } v(k) > 0; \\ -\gamma, & \text{if } v(k) < 0. \end{cases} \tag{22}$$

In order to consider the constraint on Φ when implementing these two elementary control strategies, two methods are employed:

Method 1 The magnitude of control signals are reduced to lessen the constraint violation on Φ. For bang-bang control, the magnitude of the control input signal is reduced by choosing a smaller value of γ. For linear control, either a smaller γ is chosen and/or the feedback gain F is reduced so that the constraint on Φ is satisfied. However, the simulations show that a better performance can usually be achieved by reducing the value of F alone than by reducing γ (or both γ and F together). This is because reducing γ can cause more severe input saturation, which can further degrade control performance, while reducing F leads to a smaller control signal, which can lessen or even avoid the saturation, see Fig. 6. In the simulations, $\gamma = 9 \times 10^4$ is chosen for the bang-bang control and $F = 4.5 \times 10^4$ is chosen for the linear control.

Method 2 The control signals are modified to lessen the constraint violation on Φ during the simulation period as follows: 1) the signal Φ is measured at each sampling instant; 2) if this measured Φ exceeds a predefined limit, denoted by $[-\tilde{\Phi}_{\max}, \tilde{\Phi}_{\max}]$, then the control input is set to zero, i.e., $u = 0$. Note that the value of $\tilde{\Phi}_{\max}$ is not generally the same as the actual limit of Φ; $\tilde{\Phi}_{\max}$ is purely used as a tuning parameter, and its magnitude is influenced by the wave's speed profile. In the simulations, $\tilde{\Phi}_{\max} = 0.4$ m **is tuned** for both the bang-bang control and the linear control.

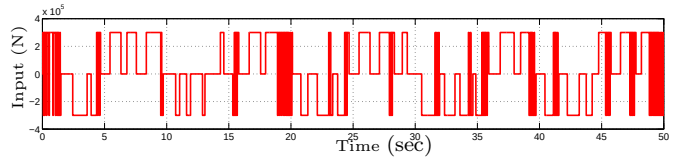

(a) Bang-bang control (method 1)

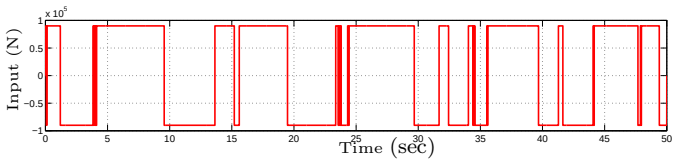

(b) Bang-bang control (method 2)

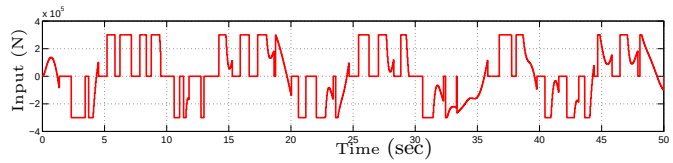

(c) Linear control (method 1)

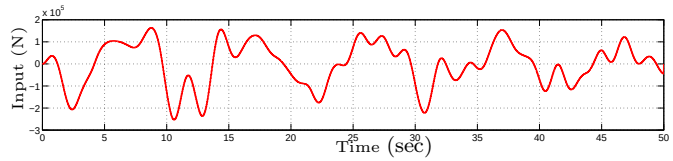

(d) Linear control (method 2)

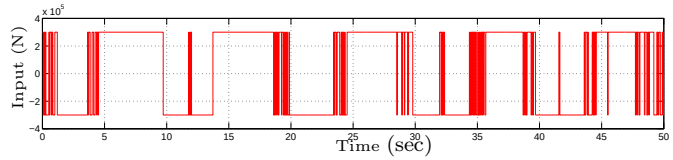

(e) DP (without prediction error)

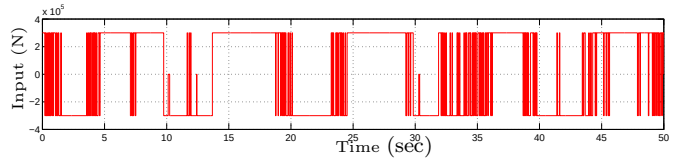

(f) DP (with prediction error)

Figure 6: The control input as a function of time. The inputs generated by all the candidate controllers satisfy the input constraint.

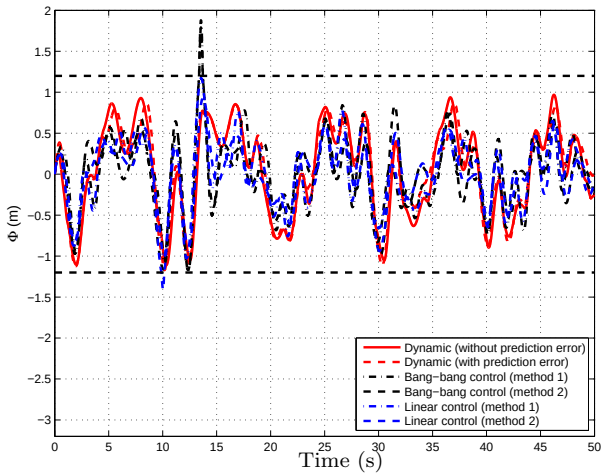

Figure 7: The vertical displacement difference between the water level and the mid-point of the float. The state constraint is satisfied for the DP control with or without prediction error and the control methods i), ii) and vi); but a constraint violation occurs for the control methods iii), iv) and v) at about 14 seconds.

In summary, the simulation results are compared in the following cases:

i) Dynamic programming without prediction error;

ii) Dynamic programming with prediction error;

iii) Bang-bang control method 1;

iv) Bang-bang control method 2;

v) Linear control method 1;

vi) Linear control method 2;

The control input signals are plotted for all the control methods in Fig. 6, and it is clear that the inputs are all limited within $[-3 \times 10^5, 3 \times 10^5]$ N. Fig. 7 shows the buoy movement displacement Φ (in meters) when using all the control methods. It can be seen that the constraint on Φ is satisfied for the cases i) ii) and vi), but not for the cases iii), iv) and v), no matter what tuning parameters are tried. Although the control methods in cases iii), iv) and v) cannot be used in reality due to the constraint violations, the simulations **are still included** here for comparison.

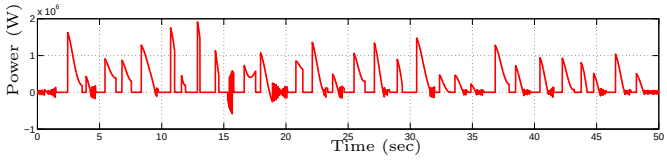

(a) Bang-bang control (method 1)

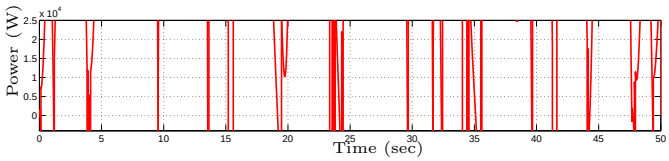

(b) Bang-bang control (method 2)

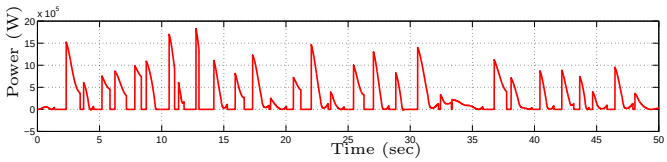

(c) Linear control (method 1)

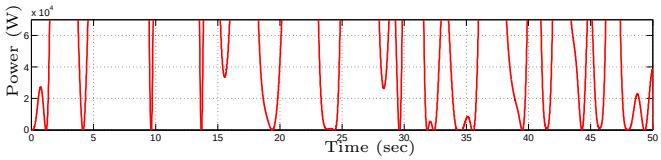

(d) Linear control (method 2)

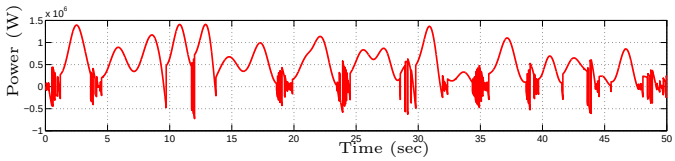

(e) DP (without prediction error)

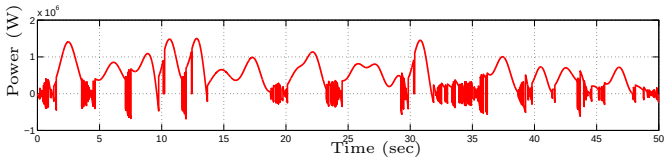

(f) DP (with prediction error)

Figure 8: Extracted power as a function of time, over 50 sec. Note that the power generated by DP control can be negative at some time instants.

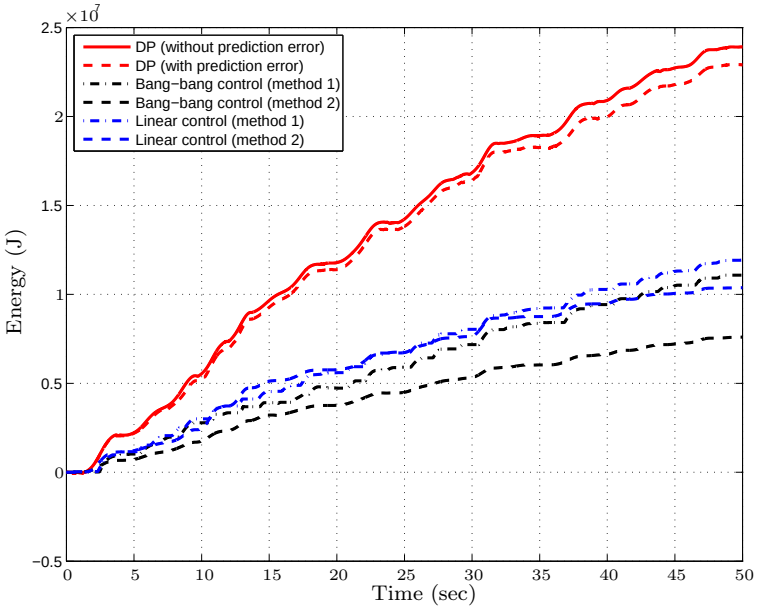

Figure 9: Extracted energy over time. **It shows** that the WEC controlled with the DP algorithm generates the most energy.

Fig. 8 shows the power generated in each case. The power generated by DP control can be negative at some time instants. The energy generated in each of the cases is plotted in Fig. 9. It can be seen that the energy generated using DP without prediction error (2.39×10^7 J) is 2 times of the amount generated using the linear control of method 2, i.e. case vi), (1.19×10^7 J). When the prediction error exists, the amount of generated energy by DP (2.30×10^7 J) is 4% less than the amount when perfect prediction is assumed. Fig. 9 demonstrates the robustness of the DP algorithm and also the importance of sea wave prediction in improving the performance of the DP control of WECs. Note that, to improve the numerical accuracy, the generated power and its integration (i.e. energy output) are both calculated by sampling the WEC continuous model at a frequency of 1000 Hz.

In practice it is possible to use the modified bang-bang control or the linear control for the small sea waves and a large limit $\Phi_{\max}$; however, it is more difficult to choose the appropriate values of $\tilde{\Phi}_{\max}$, γ and F in practice than in simulation, because these tuning parameters can vary dramatically due to the changing statistical properties of the waves. Choosing safe values would cause an extra amount of generated energy to be sacrificed.

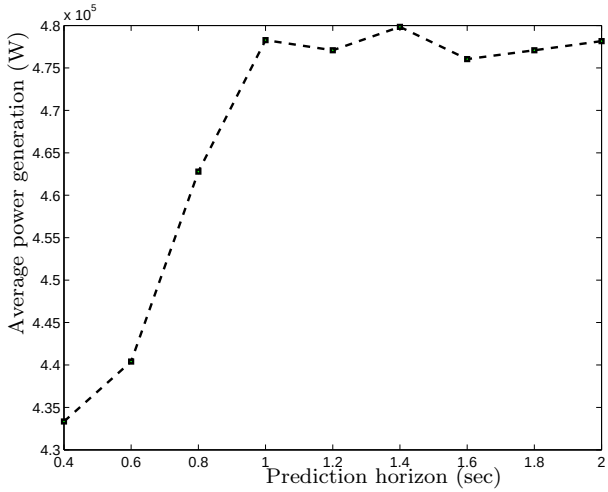

Figure 10: Average power generation at different prediction horizons assuming perfect prediction. The average power increases dramatically with the length of the prediction horizon up to about 1 second and saturates after 1 second.

5.2. The influence of prediction horizon on DP control performance

In this discussion **it is assumed** that there is no prediction error, because the results with prediction error are very similar. Fig. 10 shows the average power generation using the DP control strategy at different prediction horizons from $H_p = 0.4$ sec (corresponding to $N = 10$) to $H_p = 2$ sec (corresponding to $N = 50$). The average power is $P_{\text{avg}} = E/T$, where $T = 50$ sec and E is the energy generated during 50 sec. It can be seen that the average power increases sharply with H_p when $H_p \leq 1$ sec (corresponding to N=25), and it saturates after $H_p = 1$ sec. This means that a prediction horizon of only $H_p = 1$ sec can be used without degrading the WEC performance significantly, while reducing the computational burden.

The simulations show that the prediction horizon required to secure the majority of the benefits from optimal control is very short, typically one second. The natural conclusion is that a very short wave prediction time is required from the DSWP, so short in fact that it suggests that simple linear extrapolation from the present wave profile data should be effective. This at first appears surprising because the early work by Falnes suggested long prediction times would be required. The explanation is that Falnes' approach was to obtain an estimate of the Fourier transform $W(j\omega)$ of the incoming wave profile and then conjugate match the frequency response of the WEC

to this. Clearly this requires a long enough predictive time window to obtain a reasonable estimate of $W(j\omega)$.

The obvious conclusion would appear to be that the extra effort involved in providing DSWP is not justified in practice, suggesting that by knowing the WEC motion the wave profile can be determined. For totally linear WECs, obtaining the profile of a multi-directional sea in this manner would imply de-convoluting the WEC impulse response from the WEC motion to determine the wave system in the x, y, t domain. However the WEC motion is subject to constraints and other nonlinearities, so that it is not possible to estimate the wave profile from local data. It is necessary to use wave sensors placed sufficiently far from the WEC to minimise the effect of the wave system created by WEC motion. This distance causes a propagation delay which once more necessitates substantial prediction times, of the order of 10 seconds. Thus the conclusion is that while in principle a long prediction horizon of tens of seconds is not required for optimal WEC control, in practice it is the only way that the predictive control can be realized.

6. Conclusion

In this paper, the constrained optimal control problem of WECs is addressed. DP has been used as an on-line constrained optimal controller on a point absorber. Two other elementary control strategies are also proposed for a comparison purpose. A numerical simulation demonstrates the promising direction of using DP to control the WECs. The success of using the on-line constrained optimization technique relies on the recent development of real time sea wave prediction methods.

In future work, the following topics **are worthy of pursuing**:

1) Efficient optimal control algorithms for high order WEC models.
2) Integrating the sea wave prediction model in the controller.
3) Optimal control of a whole wave farm, taking coupling into account.
4) Experimental tests for the control algorithms.

Acknowledgments

The authors acknowledge the support of European Commission, Seventh Framework Programme, "Demonstration & Deployment of a Commercial Scale Wave Energy Converter with an Innovative Real Time Wave by Wave Tuning System (WAVEPORT)". The second author thanks the Royal

Academy of Engineering for a "distinguished visiting fellowship" that enabled him to visit Exeter in August-September 2010.

Appendix A. Quantization of the state space

Suppose $x_i \in \mathbb{X}$, with $i = 1, 2$, are evenly divided by N_{xi} points in the range of $[x_{i\,\min}, x_{i\,\max}]$, so that the length of each interval is

$$\Delta x_i = \frac{x_{i\,\max} - x_{i\,\min}}{N_{xi} - 1}.$$

For the WEC control problem, $x_{1\,\min} = -\delta$, $x_{1\,\max} = \delta$ **hold**. Since no constraint is imposed on x_2, the values of $x_{2\,\min}$ and $x_{2\,\max}$ should be chosen such that the interval $[x_{2\,\min}, x_{2\,\max}]$ is large enough to guarantee that the trajectory of x_2 is always within this range.

The grid points of $\mathbb{X} \cap \{x \in \mathbb{R}^2 \,|\, x_{2\,\min} \le x_2 \le x_{2\,\max}\}$ are

$$x_{i,t_i} = x_{i\,\min} + (t_i - 1)\Delta x_i \quad \text{with} \quad t_i = 1, \ldots, N_{xi},\ i = 1, 2$$

where the first subscript i represents the i^{th} component of x, while the second subscript t_i represents the t_i^{th} quantized value of the corresponding i^{th} state component. The set of quantized state vectors is given by

$$\mathbb{X}^Q = \left\{ x^{(j)} \,\middle|\, x^{(j)} = \begin{bmatrix} x_{1,t_1} \\ x_{2,t_2} \end{bmatrix}, \begin{array}{l} j = (t_2 - 1)N_{x1} + t_1, \\ t_1 = 1, \ldots, N_{x1},\ t_2 = 1, \ldots, N_{x2} \end{array} \right\},$$

where the superscript j represents the index of each vector in $\mathbb{X}^Q$.

Appendix B. Associating quantized state

Given a state $x(k+1) = [x_1, x_2]^\top$, the index j of the nearest point $x^{(j)} \in \mathbb{X}^Q$ can be determined by:

$$\begin{aligned} j_1 &= \lfloor (x_1 - x_{1\,\min})/\Delta x_1 + 0.5 \rfloor \\ j_2 &= \lfloor (x_2 - x_{2\,\min})/\Delta x_2 + 0.5 \rfloor \\ j &= j_2 N_{x1} + j_1 + 1. \end{aligned}$$

Here $\lfloor c \rfloor$ is used to find the largest integer smaller than $c \in \mathbb{R}$.

References

[1] J. Falnes, Ocean Waves and Oscillating Systems, Cambridge University Press, 2002.

[2] B. Drew, A. R. Plummer, M. N. Sahinkaya, A review of wave energy converter technology, Proc. IMechE Part A: J. Power and Energy 223 (2009) 887–902.

[3] S. H. Salter, Wave power, Nature 249 (5459) (1974) 720–724.

[4] S. H. Salter, Progress on Edinburgh ducks, in: IUTAM Sym. on Hydrodynamics of Ocean Wave Energy Utilisation, Springer Verlag, 1985.

[5] J. Falnes, A review of wave-energy extraction, Marine Structures 20 (4) (2007) 185–201.

[6] B. Kinsman, Wind Waves: Their Generation and Propagation on the Ocean Surface, Prentice-Hall, Englewood Cliffs, N.J., 1965.

[7] M. R. Belmont, A lower bound estimate of the gains stemming from quiescent period predictive control using conventional sea state statistics, Journal of Renewable Sustainable Energy1, article number 063104 (2009), 8 pages.

[8] M. R. Belmont, Increases in the average power output of wave energy converters using quiescent period predictive control, Renewable Energy 35 (2010) 2812–2820.

[9] K. Budal, J. Falnes, Optimum operation of improved wave-power converter, Marine Science Communciations 3 (2) (1977) 133–150.

[10] K. Budal, J. Falnes, A resonant point absorber of ocean-wave power, Nature 256 (1978) 478–479, (With Corrigendum in Vol 257, p 626.).

[11] J. Falnes, K. Budal, Wave power conversion by point absorption, Norwegian Maritime Research 6 (4) (1978) 2–11.

[12] E.L. Morris and H.K. Zienkiewicz and M.M.A. Purzanjani and J.O. Flower and M.R. Belmont, Techniques for sea state prediction, in: 2nd. Int. Conf. on Maneuvering and Control of Marine Craft, Southampton, 1992, pp. 547–571.

[13] E. L. Morris, H. K. Zienkiewicz, M. R. Belmont, Short term forecasting of the sea surface shape, Int. J. Shipbld. Prog. 45 (1998) 381–400.

[14] M. R. Belmont, J. M. K. Horwood, J. Baker, Avoidance of phase shift errors in short term deterministic sea wave prediction, Journal of Marine Engineering and Technology (3) (2003) 21–26.

[15] M. R. Belmont, J. M. K. Horwood, R. W. F. Thurley, J. Baker, Filters for linear sea-wave prediction, Ocean Engineering 33 (2006) 2332–2351.

[16] M. R. Belmont, J. M. K. Horwood, The effect of frequency distribution in simulations of deterministic sea wave prediction, Int. Shipbld. Prog. (46) (1998) 265–276.

[17] M. R. Belmont, E. L. Morris, Adaptive measurement and signal processing strategies associated with deterministic sea wave prediction, Cambridge, UK, 1994, pp. 21–26.

[18] D. R. Edgar, J. M. K. Horwood, R. Thurley, M. R. Belmont, The effects of parameters on the maximum prediction time possible in short term forecasting of the sea surface shape, Int. Shipbuild. Progr. 47 (251) (2000) 287–301.

[19] L. Abusedra, M. R. Belmont, Prediction diagrams for deterministic sea wave prediction and the introduction of the data extension prediction method, Int. J. Sipbuilding Prog. 48 (1) (2011) 59–81.

[20] I. Prislin, J. Zhang, Deterministic decomposition of deep water short crested irregular gravity waves, J. Geophys. Res. 102 (1997) 677–688.

[21] J. Zhang, J. Yang, J. Wen, I. Prislin, K. Hong, Deterministic wave model for short-crested ocean waves: Part i. theory and numerical scheme, Applied Ocean Research 21 (4) (1999) 167–188.

[22] J. Zhang, I. Prislin, J. Yang, J. Wen, Deterministic wave model for short-crested ocean waves: Part ii. comparison with laboratory and field measurements, Applied Ocean Research 21 (4) (1999) 189–206.

[23] G. Wu, Y. Liu, D. K. P. Yue, Numerical reconstruction of nonlinear irregular wave-field using single or multiple probe data, in: 15th Int. Workshop on Water Waves and Floating Bodies, Israel, 2000.

[24] T. T. Janssen, A. R. van Dongeren, C. Kuiper, Phase resolving analysis of multidirectional wave trains, in: Ocean Wave Measurement and Analysis, Proc., 4th Int. Symp. Waves, San Francisco, CA, 2001.

[25] G. Wu, Direct simulation and deterministic prediction of large-scale nonlinear ocean wave fields, Ph.D. thesis, MIT, Cambridge, MA (2004).

[26] P. Naaijen, R. Huijsmans, Real time wave forecasting for real time ship motion predictions, in: 27th International Conference on Offshore Mechanics and Arctic Engineering (OMAE), Portugal, 2008, pp. 377–387.

[27] E. Blondel, G. Ducrozet, F. Bonnefoy, P. Ferranti, Deterministic reconstruction and prediction of non-linear wave systems, in: 23rd Int. Workshop on Water Waves and Floating Bodies, Korea, 2008.

[28] P. Naaijen, R. R. T. van Dijk, R. H. M. Huijsmans, A. A. El-Mouhandiz, Real time estimation of ship motions in short crested seas, ASME, 2009, pp. 243–255.

[29] G. A. Nolan, J. V. Ringwood, W. E. Leithead, S. Butler, Optimal damping profiles for a heaving buoy wave energy converter, in: The Fifteenth Int. Offshore and Polar Eng. Conf., Seoul, South Korea, 2005, pp. 477–484.

[30] F. Fusco, J. V. Ringwood, Linear models for short-term wave forecasting, in: Proc. World Renewable Energy Conference, Glasgow, UK, 2008.

[31] M. Greenhow, S. P. White, Optimal heave motion of some axisymmetric wave energy devices in sinusoidal waves, Applied Ocean Research 17 (1997) 141–159.

[32] K. Budal, J. Falnes, T. Hals, L. C. Iversen, T. Onshus, Model experiment with a phase controlled point absorber, in: Proc. of Second Int. Symp. on Wave and Tidal Energy, Cambridge, UK, 1981, pp. 191–206.

[33] K. Budal, J. Falnes, L. C. Iversen, P. Lillebekken, G. Oltedal, T. Hals, T. Onshus, A. Høy, The Norwegian wave-power buoy project, Tapir, Trondheim, 1982, pp. 323–344.

[34] J. Falnes, Optimum control of oscillation of wave-energy converters, International Journal of Offshore and Polar Engineering 12 (2) (2002) 147–155.

[35] U. A. Korde, Latching control of deep water wave energy devices using an active reference 29 (11) (2002) 1343–1355.

[36] A. Babarit, A. H. Clément, Optimal latching control of a wave energy device in regular and irregular waves, Applied Ocean Research 28 (2006) 79–91.

[37] F. Fusco, J. Ringwood, Short-term wave forecasting for real-time control of wave energy converters, IEEE Trans. on Sustainable Energy 1 (2) (2010) 99–106.

[38] F. Fusco, J. V. Ringwood, A study on short-term sea profile prediction for wave energy applications, in: Proc. of the 8th European Wave and Tidal Energy Conf., Uppsala, Sweden, 2009, pp. 756–765.

[39] Ocean Power Technologies, Inc., PB150 PowerBuoy, http://www.oceanpowertech.com/pb150.htm (2011).

[40] A. Wacher, K. Nielsen, Mathematical and numerical modeling of the aquabuoy wave energy converter, Mathematics-in-Industry Case Studies 2 (2010) 16–33.

[41] A. A. E. Price, New Perspectives on Wave Energy Converter Control, Ph.D. thesis, The University of Edinburgh, Edingburgh, UK (2009).

[42] J. Hals, J. Falnes, T. Moan, Constrained optimal control of a heaving buoy wave-energy converter, J. of Offshore Mechanics and Arctic Engineering 133 (1) (2011) 011401.

[43] T. K. A. Brekken, On model predictive control for a point absorber wave energy converter, in: PowerTech, 2011 IEEE Trondheim, 2011, pp. 1–8.

[44] J. A. M. Cretel, G. Lightbody, G. P. Thomas, A. W. Lewis, Maximisation of energy capture by a wave-energy point absorber using model predictive control, in: Proc. 18th IFAC World Congress, Milano, 2011.

[45] R. E. Bellman, Dynamic Programming, Princeton University Press, NJ, USA, 1957.

[46] R. E. Larson, J. L. Casti, Principles of Dynamic Programming, Marcel Dekker, Inc., New York, 1978.

[47] L. S. Pontryagin, V. G. Boltyanskii, R. V. Gamkrelidze, E. F. Mishchenko, The Mathematical Theory of Optimal Processes, John Wiley & Sons, New York, 1962.

[48] E. B. Lee, L. Markus, Foundations of Optimal Control Theory, John Wiley & Sons, 1967.

[49] M. Athans, P. L. Falb, Optimal Control - An Introduction to the Theory and its Applications, McGraw-Hill, 1966.

[50] O. Sundström and D. Ambühl and L. Guzzella, On implmentation of dynamic programming for optimal control problems with final state constraints, Oil & Gas Science and Technology – Rev. IFP 65 (2010) 91–102.

[51] J.N.B.A. Perdigão and A.J.N.A. Sarmento, A phase control strategy for OWC devices in irregular seas, in: J. Grue (Ed.), The Fourth International Workshop on Water Waves and Floating Bodies, University of Oslo, Oslo, 1989, pp. 205–209.

[52] J.N.B.A. Perdigão , Reactive-control strategies for an oscillating-water-column device, Ph.D. thesis, Universidade Técnica de Lisboa, Instituto Superior Técnico (1998).

[53] A. Clément and C. Maisondieu, Comparison of time-domain control laws for a piston wave absorber, in: European Wave Energy Symposium, East Kilbride, Scotland, UK, 1993, pp. 117–122.

[54] G. Chatry and A. Clément and T. Gouraud, Self-adaptive control of a piston wave absorber, in: Eighth International Offshore and Polar Engineering Conference, Vol. 1, International Society of Offshore and Polar Engineering, Golden, Colo., 1998, pp. 127–133.

[55] L. Lasdon, A. Waren, R. Rice, An interior penalty method for inequality constrained optimal control problems, IEEE Transactions on Automatic Control 12 (4) (1967) 388–395.

[56] M. R. Belmont, J. M. K. Horwood, R. W. F. Baker, J. Baker, Shallow angle wave profiling LIDAR, Journal of Atmospheric and Oceanic Technology 24 (6) (2007) 1150–1156.

[57] R. Boudarel, J. Delmas, P. Guichet, Dynamic Programming and its Application to Optimal Control, Academic Press, New York, 1971.

[58] J. M. Maciejowski, Predictive Control with Constraints, Prentice Hall, Englewood Cliffs, NJ, 2002.

[59] D. Q. Mayne, J. B. Rawlings, C. V. Rao, P. O. M. Scokaert, Constrained model predictive control: Stability and optimality, Automatica 36 (6) (2000) 789–814.

[60] Y. Tazaki and J. Imura, Finite abstractions of discrete-time linear systems and its application to optimal control, in: 17th IFAC World Congress, Seoul, South Korea, 2008.

[61] J. N. Newman, Marine Hydrodynamics, The MIT Press, Cambridge, MA, 1977.